Geotechnical Engineering

Net load–displacement estimation in soil-nail pullout tests
Seo, Pelecanos, Kwon and Lee

ice | proceedings

Proceedings of the Institution of Civil Engineers

http://dx.doi.org/10.1680/jgeen.16.00185
Paper 1600185
Received 04/10/2016 Accepted 24/04/2017
Keywords: geotechnical engineering/models (physical)/slope – stabilisation

ice Institution of Civil Engineers publishing

Net load–displacement estimation in soil-nail pullout tests

Hyung-Joon Seo PhD
Lecturer, Department of Civil Engineering, Xi'an Jiaotong Liverpool University, Suzhou, China

Loizos Pelecanos PhD
Lecturer, Department of Architecture & Civil Engineering, University of Bath, Bath, UK

Young-Sam Kwon MSc
PhD Candidate, School of Civil, Environmental and Architectural Engineering, Korea University, Seoul, Republic of Korea

In-Mo Lee PhD
Professor, School of Civil, Environmental and Architectural Engineering, Korea University, Seoul, Republic of Korea (corresponding author: inmolee@korea.ac.kr)

Soil-nails are used to stabilise a soil mass by exploiting the resistance generated by the skin friction between the ground and grout and the tensile stiffness of the reinforcing material. A load–displacement curve is obtained from in situ pullout load tests performed by considering the elastic shear modulus and ultimate skin friction capacity between the soil and grout. This study determines the shear behaviour between the soils and grout analytically, especially the soil-dilation effect during shearing that is one of the main factors affecting the ultimate skin friction, even though this estimation is rather cumbersome. Many studies assume a full bond between the grout and the steel reinforcing bar, thus neglecting their relative displacement. In this study, the net load–displacement between the ground and grout is obtained by subtracting the nail elongation from the load–displacement of the pullout tests when estimating the shear displacement. Numerous field pullout tests are performed in this study under various ground conditions and through various construction methods. The dilatancy angles are estimated dependent on the soil type by comparing the net load–displacement curve obtained in the field with that obtained theoretically.

Notation

A	dimensionless parameter depending primarily on the nature of the soil
c	cohesion of soil
d	model parameter that dictates degradation of slope with displacement
$d_{\text{excavation}}$	displacement during excavation
d_{final}	final displacement
d_{nail}	tensile elongation of reinforcing material
d_{skin}	shear displacement between the ground and grout
E	elastic modulus of soil
f	coefficient of friction between soil and grout
G	elastic shear modulus of soil
G_{g}	shear modulus of soil resulting from gravitational grout
G_{p}	shear modulus of soil resulting from pressurised grout
K_0	coefficient of lateral earth pressure at rest
k_{max}	initial (maximum) slope of net load–displacement curve
l	embedment depth of soil-nail
n	dimensionless parameter depending primarily on current strain
P	pullout load
P_0	skin friction load under elastic conditions
p'	mean effective stress
p'_{g}	mean effective stress in gravitational grout
p'_{p}	mean effective stress in pressurised grout
p_{r}	reference pressure
r_0	radius of soil-nail
r_{m}	radial distance at which shear stresses in soil become negligible
γ	shear strain
ε	normal strain
ν	Poisson ratio of soil
ρ	factor of vertical homogeneity of soil stiffness
σ_{m}	mean normal stress
τ_{f}	ultimate skin friction of soil-nail
ϕ	internal friction angle
ψ	dilatancy angle

1. Introduction

Soil-nailing is a technique used to improve the stability of earth structures by inserting a reinforcing material and grout into the ground (NHI, 2015). It is a passive method because resistance occurs only during ground movement. It has two main resistance components: (*a*) skin friction between the ground and grout and (*b*) tensile stresses of the reinforcing material. Pullout tests are performed to verify the contributions of these two factors. The results from these tests show the relation between the pullout load and the displacement. However, these results cannot distinguish between the contributions made by each component. The slope and yield point of the load–displacement curve depend on the ground conditions. The shear displacement between the ground and grout in loose soil predominantly occurs when the ultimate skin friction is far smaller than the tensile strength of the reinforcing

material. In contrast, the tensile displacement of the reinforcing material in dense soil dominates the displacement when the ultimate skin friction is larger. Therefore, it is important to estimate the relative contributions of each resistance component in the design.

Two methods can be adopted to improve the design load of a soil-nail system: (*a*) increase the skin friction between ground and grouting, for example, through pressurised grouting (Seo *et al*., 2012) and (*b*) increase the tensile stress of the reinforcing material, for example, through hybrid methods in which the soil-nail and anchoring are combined. It is possible to determine the reinforcing effect for the latter from a simple calculation of the material properties. However, it is difficult to verify the reinforcing effect for the former in each ground because the ultimate skin friction and shear modulus of the soil change with different ground conditions. If the shear strength from the Mohr–Coulomb criteria is used to verify the shear of a soil-nail, it is possible to underestimate the ultimate skin friction because soil dilation is not considered. Therefore, the Japan Geotechnical Society (JGS, 2000) empirically proposed the ultimate skin friction (τ_f) based on the standard penetration test (SPT)-*N* value. Wang and Richwien (2002) suggested a theoretical equation that considers soil dilation to obtain the ultimate skin friction. Seo *et al*. (2012) modified this theoretical solution to make it suitable for use with cohesive soils. However, it is not easy to estimate the dilatancy angle of soil. Pyke (1979) studied non-linear soil models for irregular cyclic loadings. Randolph and Wroth (1978) also suggested a theoretical solution to determine the stiffness of the soil, which is estimated from the load transfer (*t*–*z*) curves. Several pressuremeter tests (PMTs) were performed in this study to define the elastic shear behaviour of the soil.

The load–displacement curve obtained from the pullout test cannot be compared directly with the theoretical solution because this load–displacement curve includes the effect of steel bar elongation. However, it is possible to estimate the net load–displacement between the ground and grout by subtracting the nail elongation when estimating the shear displacement from the load–displacement curve obtained from the pullout tests. A number of field pullout tests were performed in this study under various ground conditions and construction methods, and the net load–displacement curves obtained in the field are compared with those obtained from the theoretical solution.

Generally, it is assumed that there is no relative displacement between the grout and the steel bar. In this study, the relative displacement between the grout and the steel bar is also considered by comparing the strains measured in the grout with those in the nail. The resisting contribution of the skin friction component as compared to that of the steel bar can also be derived.

2. Net load–displacement curve between ground and grout

The soil-nail provides a passive structure whereby the resistance created by the soil-nail is mobilised when ground displacement adjacent to the soil-nail occurs in advance. The downward movement of the ground at the potential failure plane during the slope excavation will mobilise the resistance in the soil-nail (see Figure 1). Tan and Chow (2004) classified the soil-nail failure modes of ground inside the slope as pullout failure, shear failure and face failure. Based on these modes, the behaviour of soil-nails is divided into two types: associated behaviour and non-associated behaviour. The non-associated behaviour refers to the dominant resistance of the soil-nail, which is generated either by the tensile load of the reinforcing material or by the skin friction between ground and grout. If the tensile load of the reinforcing material is much smaller than the skin friction, shear failure occurs because the reinforcing material is subject to tensile load up to failure (Figure 1(a)). On the contrary, tensile failure in the reinforcing material occurs only to a limited extent if the skin friction is smaller than the tensile strength of the reinforcing material, and the relative displacement between the ground and grout increases significantly, causing pullout failure (Figure 1(b)).

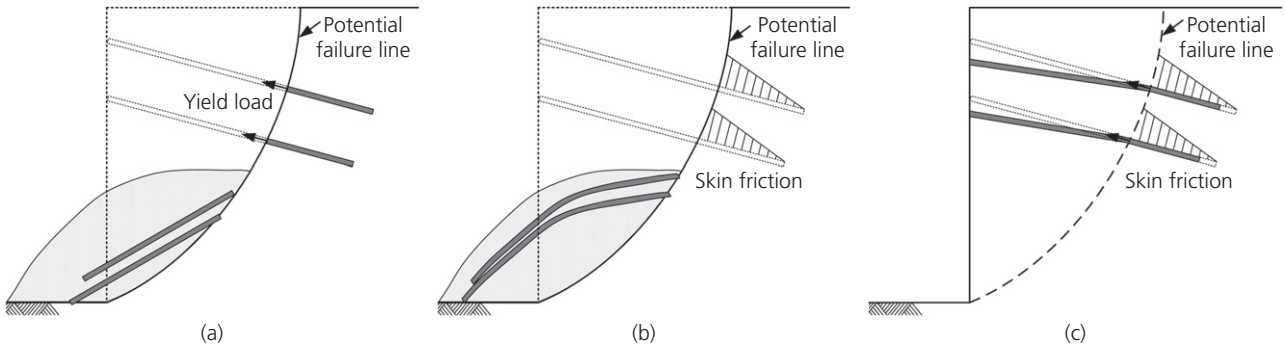

Figure 1. Soil-nail behaviour: (a) non-associated behaviour (shear); (b) non-associated behaviour (pullout); (c) associated behaviour

The reinforcing effect of soil-nailing can be maximised by utilising the resistance of the skin friction between the ground and grout and by the tensile load of the reinforcing material simultaneously; the simultaneous functioning of these two resisting factors is referred to as associated behaviour (Figure 1(c)). In other words, while the tensile elongation occurs because of the resistance of the reinforcing material, the shear displacement also causes skin friction mobilisation. The Korea Infrastructure Safety Corporation (KISC, 2006) suggests the use of a soil-nail length of 3 m in pullout tests, as this length can demonstrate the associated behaviour more effectively.

Seo *et al*. (2014) suggested three different displacement modes of soil-nails. The displacement during excavation ($d_{\text{excavation}}$) occurs first as the horizontal stress is released at the excavation side. After installing the soil-nail in the borehole, tensile elongation of the reinforcing material (d_{nail}) occurs because of the pullout load acting on the reinforcing material if the ground moves along the potential failure plane. In addition, the load acting on the reinforcing material is resisted by the skin friction between the ground and grout, causing shear displacement (d_{skin}). Therefore, the final displacement (d_{final}) is given by Equation 1.

$$1. \quad d_{\text{final}} = d_{\text{excavation}} + d_{\text{nail}} + d_{\text{skin}}$$

The displacement during excavation ($d_{\text{excavation}}$) can be estimated easily if the elastic modulus of the ground (E_{ground}) is known. In addition, the tensile elongation of the reinforcing material (d_{nail}) can be calculated easily with the known value of the elastic modulus of the reinforcing material (E_{steel}). However, it is not easy to predict the shear displacement between the ground and the grout (d_{skin}). Therefore, the shear behaviour between the ground and the soil-nail is theoretically derived in this study and field pullout tests are performed to verify the theory.

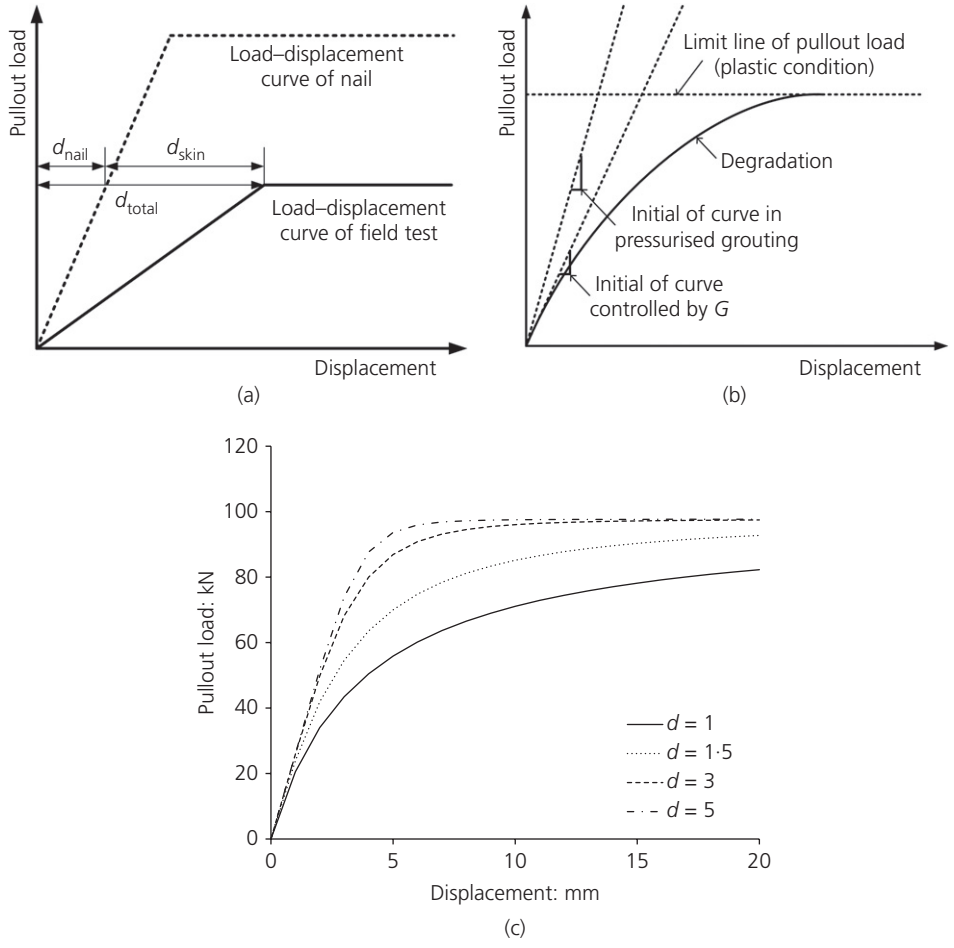

Figure 2. Theoretical net load–displacement curve: (a) net displacement = d_{skin}; (b) description of net load–displacement curve; (c) effect of degradation parameter, d

A simplified load–displacement curve (assuming an elastic–perfectly plastic behaviour) is shown in Figure 2(a). The displacement in the load–displacement curve from the pullout test shown in Figure 2(a) is obtained by adding the tensile elongation of the reinforcing material to the shear displacement between the ground and the grout. The load–displacement curve of the reinforcing material (nail) can then be estimated directly, as shown in Figure 2(a), as it will show elastic behaviour. Therefore, it is possible to estimate the net load–displacement curve by subtracting the nail elongation when estimating the shear displacement from the load–displacement curve obtained from the pullout tests.

Soil deformation is highly non-linear and differs significantly from the deformation of a linear elastic material or bilinear elastic–perfectly plastic material. The non-linear behaviour of the soil–structure interaction (such as the behaviour of piles and/or soil-nails) can be represented by non-linear load-transfer curves when the soil is represented by springs. This curve is usually assumed to follow a modified hyperbolic (Pyke, 1979) relation and requires three main parameters to be defined in their simple forms (see Figure 2(b)): (*a*) the initial (tangential) slope of the curve, that is, stiffness; (*b*) the ultimate value of the load (or friction); and (*c*) the degradation behaviour of the slope (i.e. how the stiffness degrades with the induced strain or displacement). Such a non-linear relationship is given by Equation 2, which requires these three aforementioned distinct parameters to be defined.

$$2.\quad P = \frac{k_{\max}}{\sqrt[d]{1 + (k_{\max}/\tau_f)^d}} 2\pi r_0 l$$

where P is the pullout load; $k_{\max}$ is the initial (maximum) slope of the curve; l is the embedment depth of the soil-nail; r_0 is the radius of the soil-nail; τ_f is the ultimate value of the skin friction of the soil-nail; and d is a model parameter that dictates the degradation of the slope with the displacement. The parameters $k_{\max}$, τ_f and d can vary with depth.

Ideally, the model parameters should be determined from the properties of the surrounding soil. Analytical or empirical relationships can be employed in such cases to define the values of $k_{\max}$ and τ_f; the effect of grout should also be considered in some cases. The latter two parameters ($k_{\max}$ and τ_f) in this study are defined based on the known material properties and by adopting theoretical relationships. The parameter $k_{\max}$ is defined using the relationship proposed by Randolph and Wroth (1978), whereas τ_f is defined using that proposed by Seo *et al.* (2012). After Randolph and Wroth (1978) the skin friction of an axially loaded pile can be expressed as

$$3.\quad P_0 = \left[\frac{G}{\ln(r_m/r_0)} 2\pi l\right] d_{skin}$$

where P_0 is the skin friction load under elastic conditions; G is the elastic shear modulus of soil; and r_m is the radial distance at which the shear stresses in the soil become negligible. Then, $k_{\max}$ can be expressed as

$$4.\quad k_{\max} = \frac{G}{\ln(r_m/r_0)} 2\pi l$$

Randolph and Wroth (1978) suggested the following value of r_m

$$5.\quad r_m = 2{\cdot}5 l\rho(1 - \nu)$$

where ρ is the factor of the vertical homogeneity of soil stiffness ($\rho = G$ at nail mid-depth/G at nail tip) and ν is the Poisson ratio of the soil. Equation 4 represents the maximum value of the stiffness of the net load–displacement of the soil-nail with gravitational grout. However, the stiffness is affected by the increase in the mean normal stress when pressurised grout is applied (see Seo *et al.*, 2012) during the injection. Viggiani and Atkinson (1995) studied the elastic shear modulus variation caused by the mean normal stress, as shown in Equation 6

$$6.\quad \frac{G}{p_r} = A\left(\frac{p'}{p_r}\right)^n$$

where p' is the mean effective stress; p_r is the reference pressure; and the dimensionless parameters A and n depend primarily on the nature of the soil and current strain, respectively. Equation 6 can be modified for use in the gravitational and pressurised grout methods as follows

$$7.\quad \frac{G_g}{p_r} = A\left(\frac{p'_g}{p_r}\right)^n$$

and

$$8.\quad \frac{G_p}{p_r} = A\left(\frac{p'_p}{p_r}\right)^n$$

where p'_g is the mean effective stress in gravitational grout and p'_p is the mean effective stress in pressurised grout. The relation of elastic shear modulus between the pressurised grout and gravitational grout can be expressed by these two equations as follows

$$9.\quad G_p = \left(\frac{p'_p}{p'_g}\right)^n G_g$$

where G_p is the shear modulus of soil resulting from pressurised grout and G_g is that of gravitational grout. The elastic shear modulus induced by pressurised grout can be calculated

from Equation 9 if the difference in the mean effective stresses between two different grout types can be determined.

Seo *et al*. (2012) suggested the ultimate skin friction of a soil-nail in cohesive soil utilising the initial suggestion proposed by Wang and Richwien (2002), as shown in Equation 10.

$$\tau_f = \frac{f}{\{1 - [2(1+\nu)/(1-2\nu)(1+K_0)]f\tan\psi\}}\sigma_m + c \quad (10)$$

Table 1. Assumed parameters for parametric studies

Length of soil-nail: m	Diameter of soil-nail: m	Coefficient of earth pressure	Poisson ratio	Unit weight: kN/m^3
3	0·13	0·5	0·34	20

where f is the coefficient of friction between soil and grout ($f = \tan\phi$); K_0 is the coefficient of lateral earth pressure at rest, assumed to be $(1 - \sin\phi)$; ψ is the dilatancy angle; σ_m is the mean normal stress; and c is the cohesion of soil. The net load–displacement curve shown in Figure 2(b) can be obtained using Equation 2 in which Equation 10 is used for τ_f, and Equation 4 is used for k_{max}. The shear modulus G in Equation 4 can be obtained from results of the pressuremeter test. The degradation parameter d is related to the elastic stiffness degradation, and ideally, it should be obtained from the stiffness degradation curves, that is, G or E with respect to γ (shear strain) or ε (normal strain). It can be determined by curve fitting utilising the results of pullout tests (see Figure 2(c)).

A parametric study to obtain the net load–displacement curve using Equations 2, 4, and 10 is performed to assess the effect of each soil parameter on the shape and limit of the curve. The

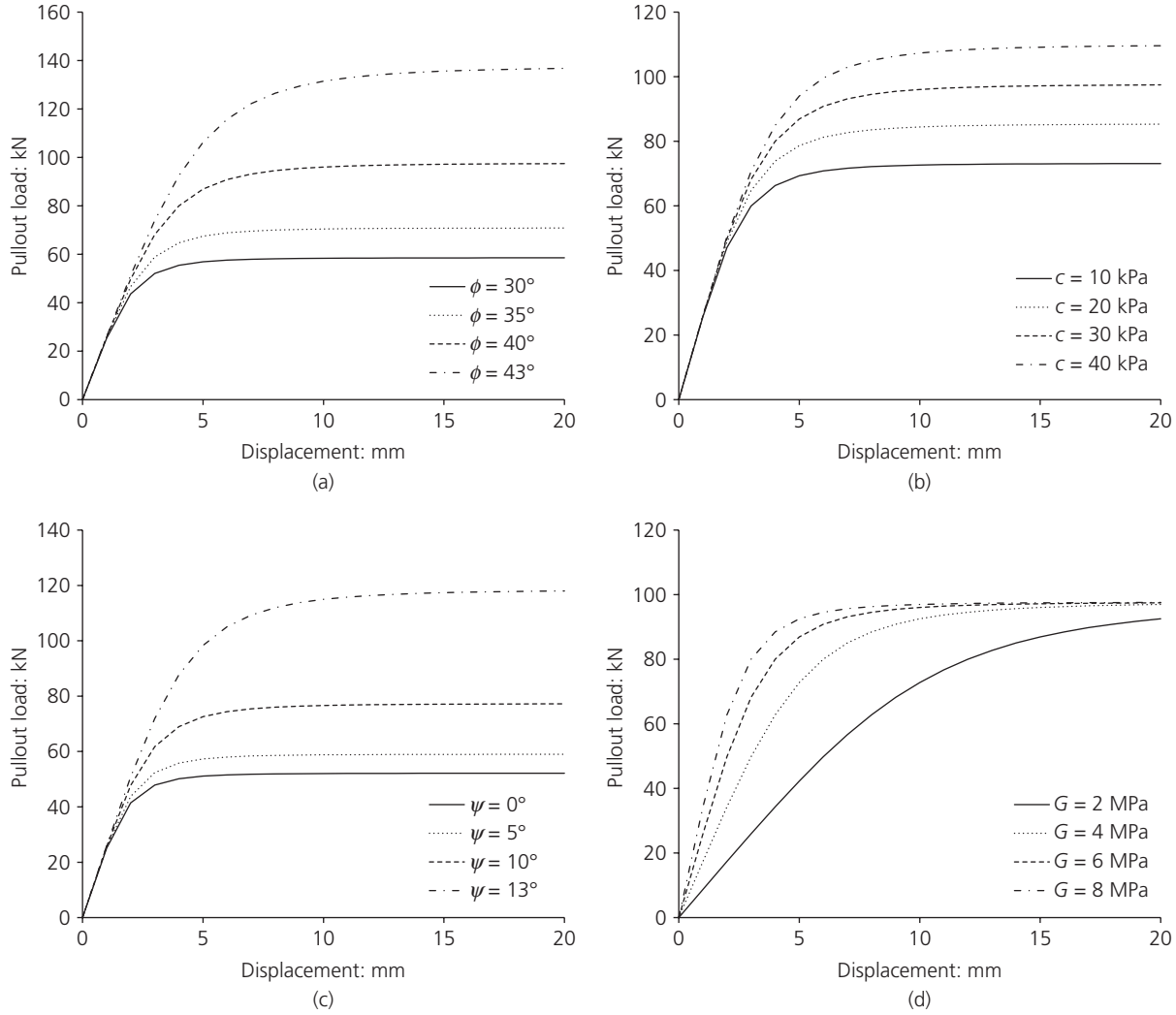

Figure 3. Parametric studies on net load–displacement curves – evaluation of the effects of different parameters: (a) variation of internal friction angle ($c = 30$ kPa); (b) variation of cohesion ($\phi = 40°$); (c) variation of dilatancy angle; (d) variation of elastic shear modulus

assumed parameters needed to perform the parametric studies are shown in Table 1. As is obvious from the Figures 3(a) and 3(b), the shear strength of soils (friction angle and cohesion) is the controlling factor affecting the ultimate pullout load. The dilatancy angle is another important parameter used to estimate the ultimate pullout load, as shown in Figure 3(c). Therefore, it is possible to seriously underestimate the ultimate pullout load if the dilation effect of soil is not considered. Figure 3(d) shows the net load–displacement curve variation induced by the variation of the elastic shear modulus. The figure shows that the slope of the net load–displacement curve is controlled mainly by the elastic shear modulus of the surrounding soil. It is necessary to find a way to increase the elastic shear modulus of the ground when intending to reduce the displacement of the soil-nail system. Pressurised grout might be a method that can be used to improve the stiffness.

3. Field pullout test to estimate net load–displacement curve

Field pullout tests were performed to verify the theoretical net load–displacement curve proposed in the previous section (see Figure 2) and investigate the effect of soil dilation. An overview of the tests is shown in Figure 4. The net load–displacement curve is dependent on the ground conditions. Therefore, three job sites which have different soil types were chosen: colluvial soil, weathered granite soil and filled soil. Two different construction methods were also chosen: gravitational grout and pressurised grout (refer to Seo *et al*. (2012) for details of pressurised grout). Three different bonded lengths (2·0 m, 3·0 m and 4·0 m) were used in the weathered granite soil to verify the nail length effect, as shown in Table 2.

In the pullout tests on colluvial soil and weathered granite soil, a 0·5 m long packer was installed along with bonded length of 2·0 m to compare gravitational grout with pressurised grout. Nails with lengths of 3·0 m and 4·0 m were used to compare the effect of different bonded lengths. In addition, vibrating wire strain gauges (VWSGs; SG 4150 and SG 4200 manufactured by Geokon) were installed by using steel wires to fix the gauges beside the steel bar. In total, seven VWSGs were installed in the soil-nail that was installed in weathered granite soil, as shown in Figures 4(b) and 4(c), to determine the relative movement between the steel and the grout. The steel strain gauges were covered with a cap to prevent the penetration of the grout. All types of soil-nails were installed in the vertical direction and the steel bar was pulled out in order to simulate the pullout test. Photographs of the three test sites are shown in Figure 5.

The main purpose of this study is to compare the theoretical solution with the load–displacement curve observed in the field pullout test. The ground properties are determined from the grain-size distribution tests, field density tests, liquid limit tests, plastic limit tests and direct shear tests shown in Table 3. These soil properties shown in Table 3 are used for the input soil parameters of the theoretical solution.

In this paper, the variation of shear modulus is required to define the entire load–displacement curve. Therefore, PMTs were performed at each site to estimate the elastic modulus of each soil. The elastic modulus of each soil can be estimated at 1·0 m and 3·0 m depths based on the results shown in Figure 6: 3·567 GPa and 8·667 GPa in colluvial soil; 5·626 GPa and 7·616 GPa in weathered granite soil; and 2·733 GPa and 5·081 GPa in filled soil, at 1·0 m and 3·0 m depths, respectively. The averaged elastic modulus can be used to determine the elastic shear modulus: 6·121 GPa in colluvial soil; 5·626 GPa in weathered granite soil; and 3·907 GPa in filled soil. The elastic shear modulus of each soil type is used for obtaining the slope of the net load–displacement curve from the proposed theory.

4. Laboratory chamber test

The mean normal stress σ_m is an important factor for obtaining the ultimate skin friction using Equation 10. As shown in Table 2, two different grout methods were adopted for colluvial and weathered granite soil. Pressurised grout offers the advantage of providing higher mean normal stress compared with that provided by the gravitational grout. Laboratory chamber tests were performed in order to determine the increase in the mean normal stress achieved by adopting the pressurised grout. The tested soils were taken from the site in which the field tests were performed, namely, colluvial and weathered granite soils. Seo *et al*. (2012) studied the behaviour of pressurised grout using a cylindrical chamber to simulate the in situ ground condition (see Figure 7(a)). Each soil type was compacted initially in this chamber test, as shown in Figure 7(b), except for an artificial borehole with a 0·1 m dia. in which the grout injection was applied. After compaction, the chamber cover was closed and the grout was then injected. A grout pressure of approximately 450 kPa was applied and controlled by a regulator, as shown in Figure 7(c), and the propeller was used to prevent the solidification of the cement. An overburden pressure of 4·0 m depth was applied at the bottom of the chamber and was controlled by the regulator. Figure 7(d) shows the earth pressure cell location used to measure the grout pressure variation.

The results measured by the earth pressure cell are shown in Figure 7(e). The grout pressure continuously increases initially during the grout injection and then the pressure is maintained for several minutes. The grout pressure then starts to decrease because of the hydration effect. The water is then released from the cement paste, and it penetrates through the soil so that the grout pressure dramatically decreases and then converges to the residual stress (Seo *et al*., 2012). The residual stress for both the colluvial and weathered granite soils was almost 20% higher than the overburden pressure. These results can be used for calculating the ultimate skin friction in

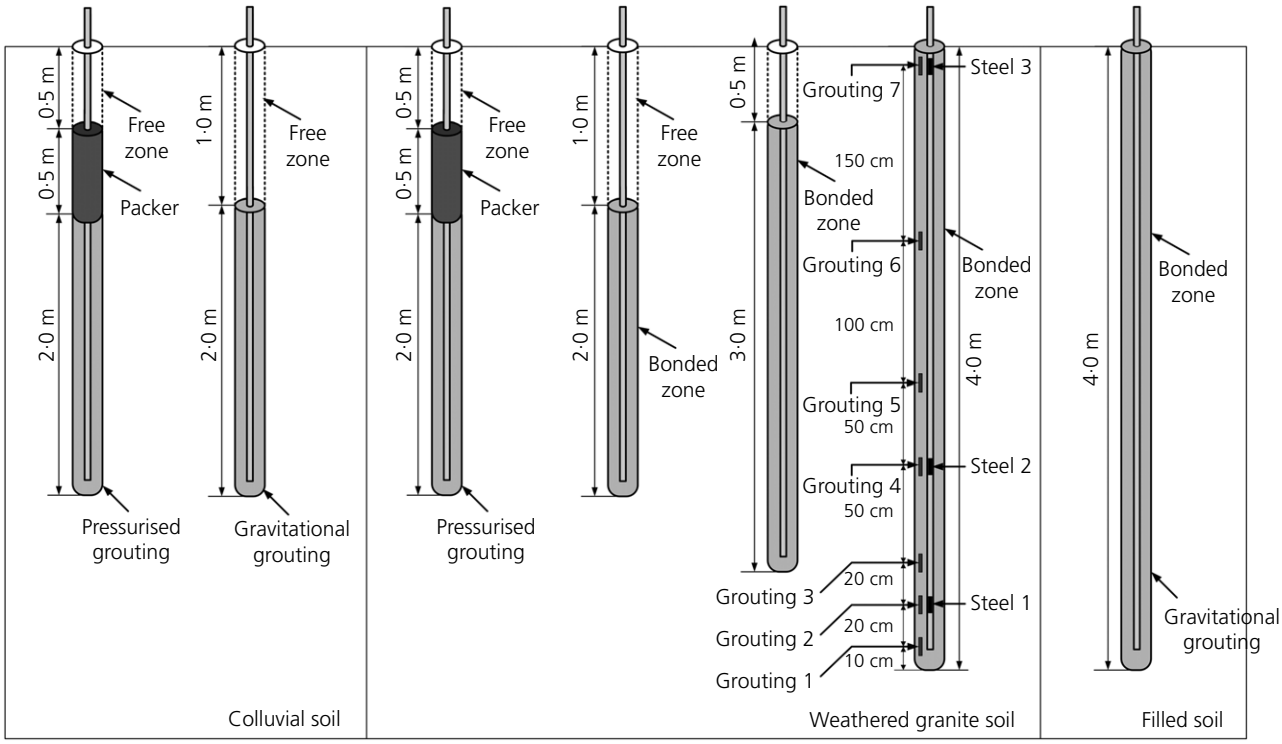

(a)

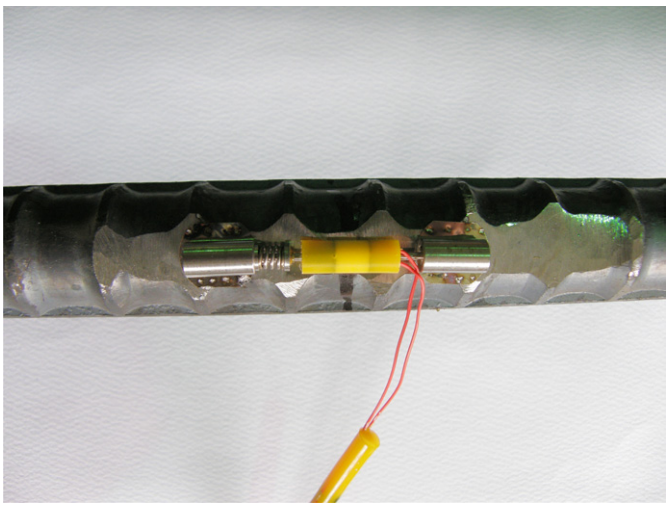

(b)

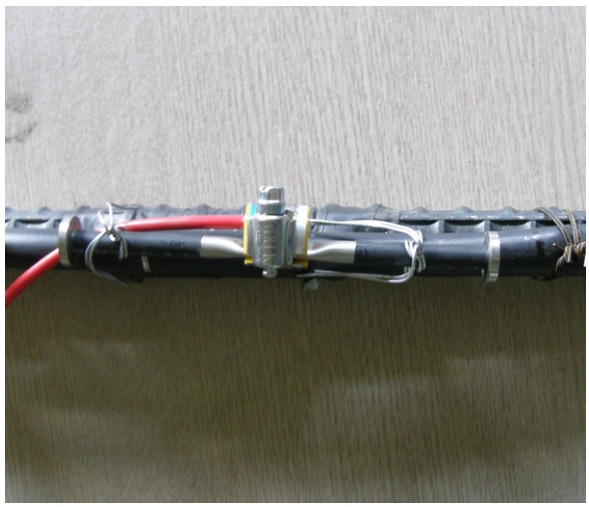

(c)

Figure 4. Overview of pullout tests: (a) soil-nail installations; (b) steel strain gauge; (c) grout strain gauge

Table 2. Overview of field pullout test

Type	Bonded length: m	Gravitational grout	Pressurised grout
Colluvial soil	2·0 (Packer: 0·5)	Three times	Three times
Weathered granite soil	2·0 (Packer: 0·5)	Three times	Three times
	3·0	Three times	—
	4·0	Three times	—
Filled soil	4·0	Three times	—

Equation 10. In addition, Equation 9 can be expressed as shown below based on these results (i.e. $p'_p \approx 1{\cdot}2p'_g$)

$$G_p = (1{\cdot}2)^n G_g \quad (11)$$

where $n = 0{\cdot}65$, as suggested by Viggiani and Atkinson (1995). The shear modulus of pressurised grout can be calculated using Equation 11: 8·011 GPa in colluvial soil and 7·616 GPa in weathered granite soil.

(a)

(b)

(c)

Figure 5. Pullout test sites: (a) colluvial soil site, Wonjoo; (b) weathered granite soil site, Busan; (c) filled soil site, Seoul

5. Results of field pullout test and verification of theoretical solution

Field pullout tests are performed to verify the effectiveness of the theoretical solution in obtaining the net load–displacement curve shown in Figure 2. Thus, the elongation that occurred in the steel bar is subtracted from the total load–displacement curve directly obtained from the field pullout test, as shown in Figure 8(a), to compare the values calculated from theory to those achieved from field pullout tests. These net load–displacement curves are compared with the results of the theoretical solution to back-calculate the dilatancy angle.

The results for the colluvial soil are shown in Figure 8(b). Two different grout methods are compared by comparing the coefficient of stiffness, which is defined as the initial slope of the net load–displacement curve. According to the results, the coefficient of stiffness of pressurised grout increases by 45·5% compared to that of gravitational grout. The main reason for the greater stiffness in the case of the pressurised grout is the increase of the mean normal stress as well as the stronger bond between the ground and grout. In contrast, the slope of the net load–displacement curve is gentle in the case of the gravitational grout because the shear displacement between the ground and grout is more dominant than the tensile elongation of the steel bar itself. The pullout load of pressurised grout also increases by 25·39% compared to that of gravitational grout. The cavity expansion that occurs when subject to pressurised grout is the main reason for the increased pullout resistance; the diameter of the grout as well as the mean normal stress surrounding the grouted area will increase because of cavity expansion (Seo *et al.*, 2012). After pullout tests, diameters of soil-nails were measured and it was found that the effect of increase in diameter is similar to previous studies (Seo *et al.*, 2012): the diameter is around 13 cm in gravitational grout and 16 cm in pressurised grout. Increased diameters were considered in the analysis.

The net load–displacement curves of the weathered granite soil are shown in Figure 8(c). The slope of the load–displacement curve of the weathered granite soil is steeper and closer to the load–displacement curve of the steel bar compared with that of the colluvial soil. The ultimate pullout loads observed for weathered granite soil are greater than those observed for colluvial soil by 34·36% in gravitational grout and 39·15% in pressurised grout. Cohesion plays the dominant role in the initial shear behaviour, but the internal friction angle becomes more dominant as shear displacement increases.

Table 3. Ground properties

Type	Cohesion: kPa	Internal friction angle: deg	Passing no. 200 sieve: %	Unified soil classification	Unit weight: kN/m^3
Colluvial soil	26·1	38	53·47	ML	18·9
Weathered granite soil	20·4	41	48·57	SM	19·5
Filled soil	12·7	34	37·00	SC	17·9

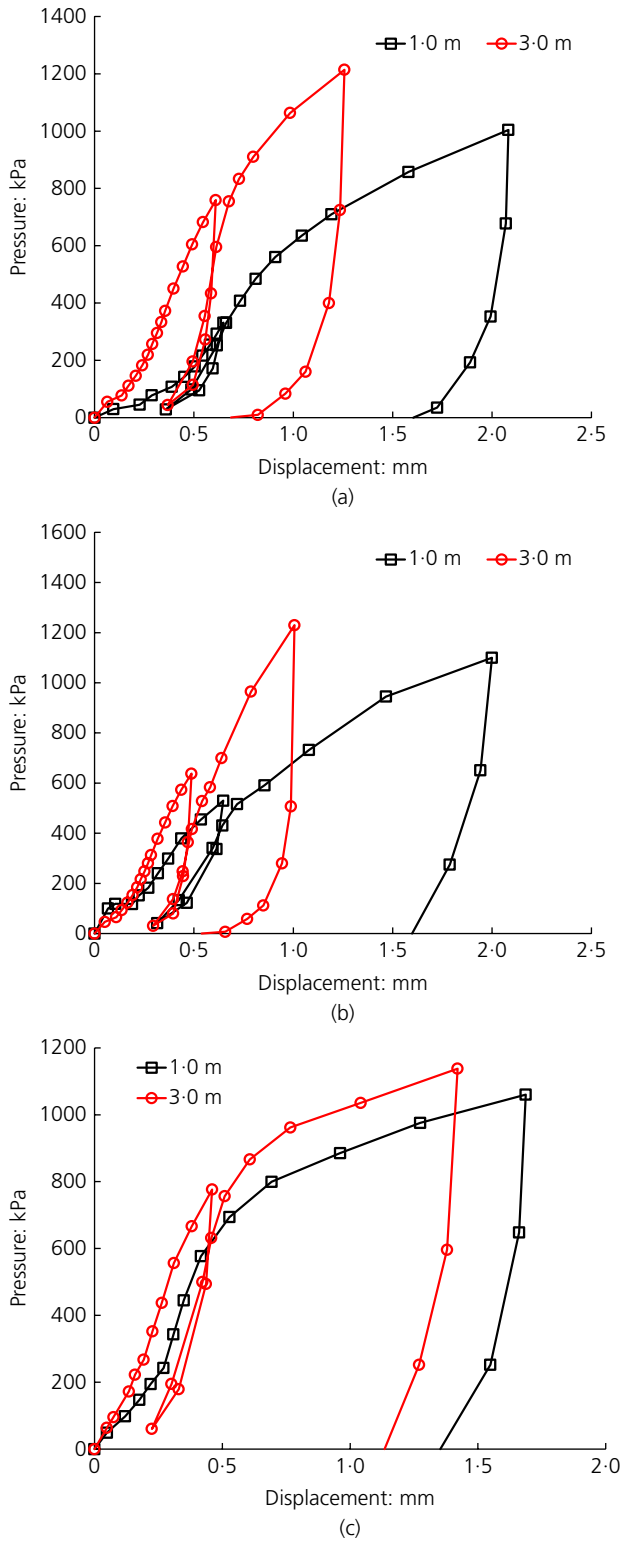

Figure 6. Pressuremeter test results: (a) colluvial soil; (b) weathered granite soil; (c) filled soil

Table 4. Back-calculated dilatancy angles

Soil conditions	Colluvial soil	Weathered granite soil	Filled soil
Dilatancy angle: deg	13·2	11·9	15·0

The net load–displacement curve of filled soil is shown in Figure 8(d). Even though the bonded length of the filled soil is 4·0 m, the slope of the net load–displacement curve is gentle and the ultimate load is small because it has low cohesion and a small internal friction angle.

The dilatancy angle of each soil condition can be obtained by fitting the theoretical solutions to the results of the field pullout tests when the soil-nail reaches the plastic state, as shown in Figures 8(b)–8(d). Table 4 shows the back-calculated dilatancy angles. The results shown in Table 4 can be used as an initial estimate when Equation 10 is used to obtain the ultimate skin friction for soil-nail design. The back-calculated dilatancy angle of 11·9° for weathered granite soil is found to be within the ranges from 9·2° to 12·3° obtained by Seo *et al.* (2012).

Figure 9 shows the net load–displacement curves of the 2·0 m, 3·0 m and 4·0 m bonded nail lengths for weathered granite soil. As the bounded length of soil-nail increases, the initial slope of the curve (i.e. the coefficient of stiffness) becomes stiffer. If the bonded length increases infinitely, the coefficient of stiffness may increase dramatically; in this case, the displacement of the soil-nail will be caused mainly by the tensile elongation of the steel bar. As the pullout load for the 4·0 m bonded nail length increases, the steel bar yields before the occurrence of the skin friction failure between ground and grout. This means that the non-associated behaviour, that is, shear failure, occurs, as shown in Figure 1(a), and the structural capacity of the reinforcing material governs the slope stability. In contrast, the pullout failure in the case of the 2·0 m bonded nail length would occur before the steel bar reaches the yield load, as shown in Figure 1(b). The bonded capacity between the ground and grout governs the slope stability in this case. The associated behaviour might occur where the tensile elongation of the reinforcing material and the shear displacement between the ground and grout occur simultaneously if the soil-nail is constructed with the bonded length of 3·0 m.

One of the ways to reduce the displacement when subject to pullout load is to adopt pressurised grout. The effect of the pressurised grout on the net load–displacement curve in the case of the weathered granite soil is shown in Figure 10. The net load–displacement curve of the 2·0 m bonded nail length with pressurised grout is equivalent to that of the 3·0 m bonded nail length with gravitational grout.

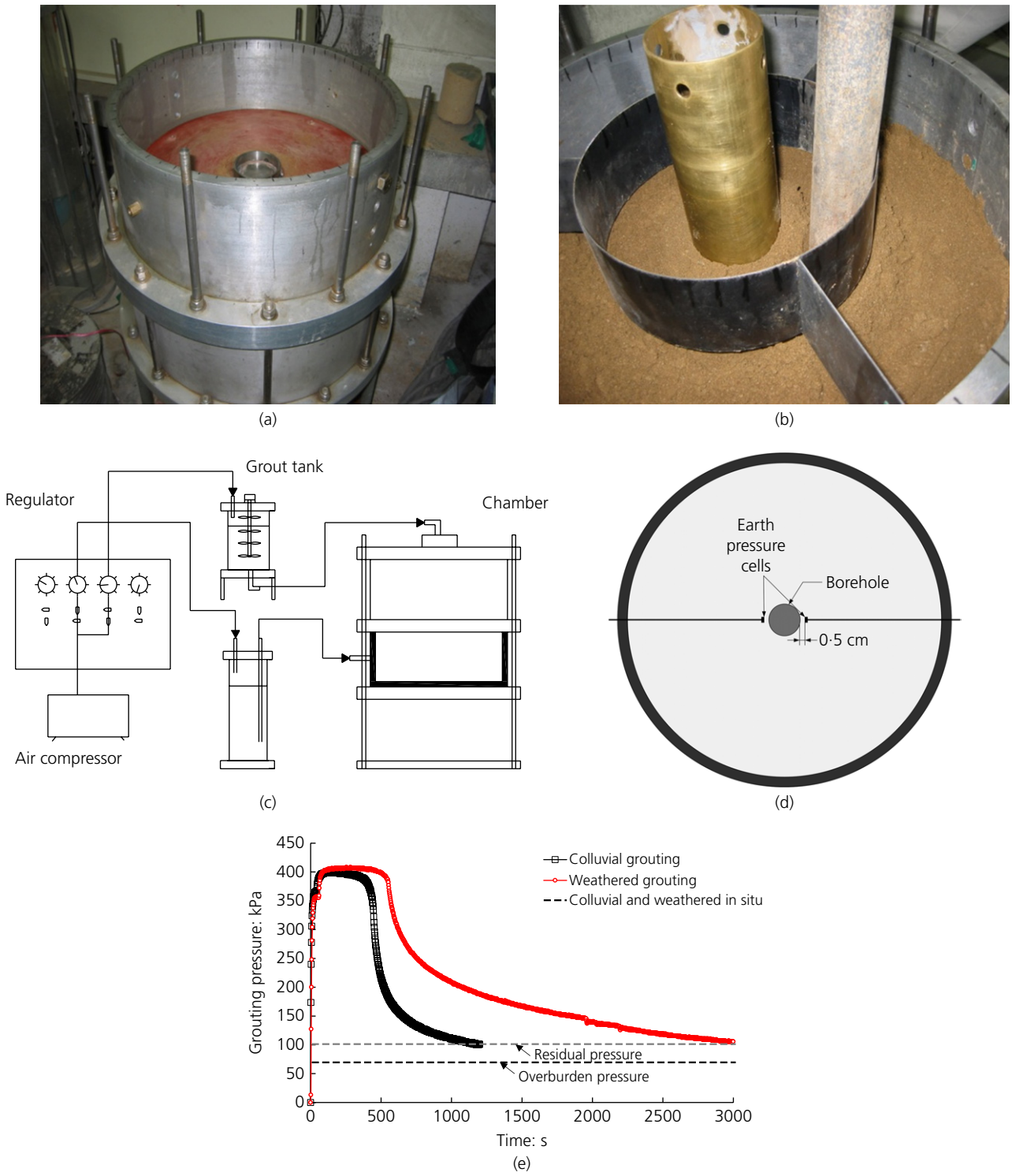

Figure 7. Laboratory chamber test: (a) chamber; (b) compaction of soil; (c) overview of chamber test; (d) earth pressure cell location; (e) grout pressure variation with time

The movement between the soil and grout is compared with the total pullout displacement as the pullout load increases (see Figure 11) in order to determine the portion of shear displacement that occurs. Figure 11(a) shows the effect of pressurised grout on the shear displacement portion. The shear displacement portion of pressurised grout for the colluvial soil is

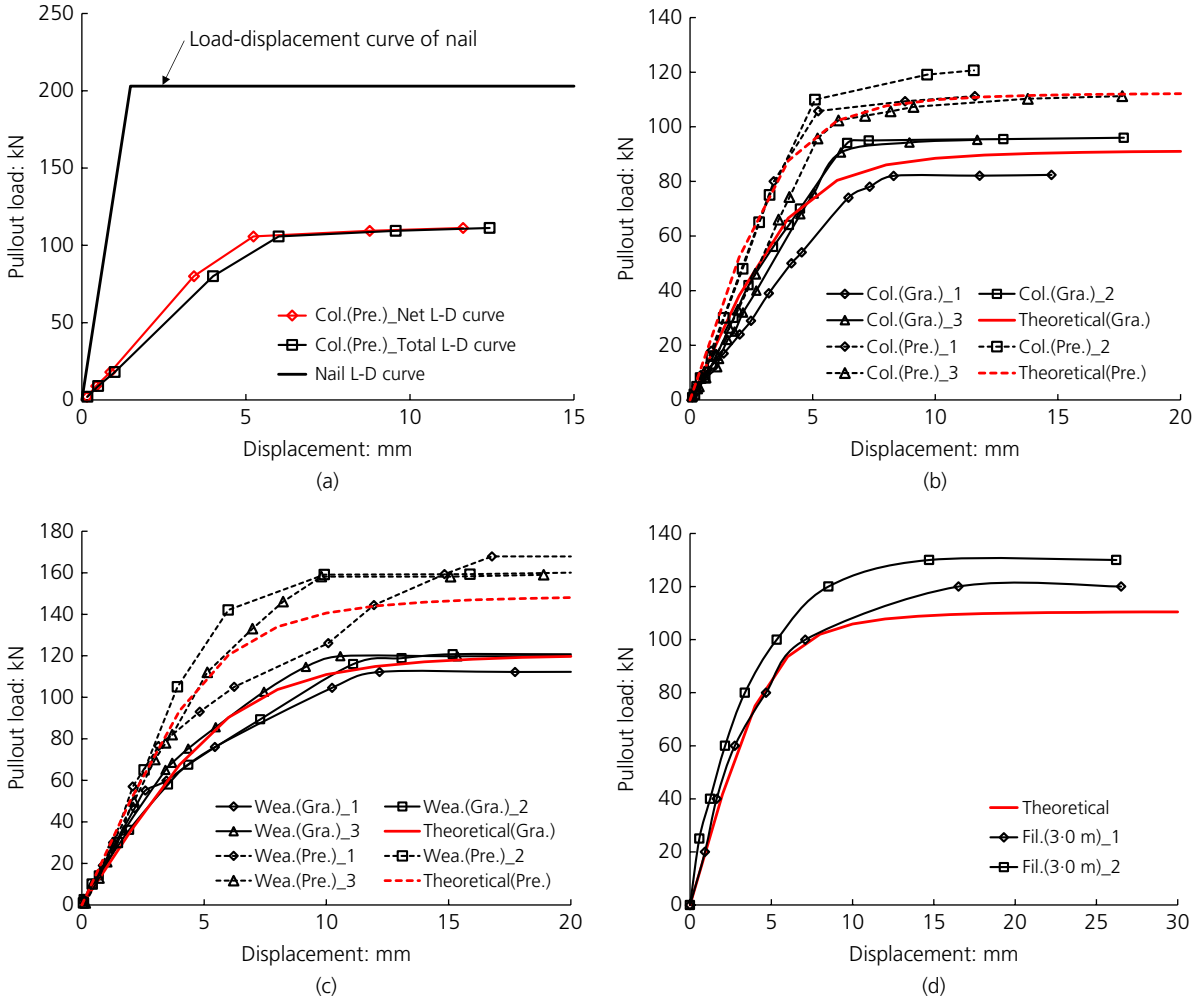

Figure 8. Net load–displacement curves from field pullout test and theoretical solution: (a) example to obtain net load–displacement curve; (b) colluvial soil; (c) weathered granite soil; (d) filled soil (Col., colluvial soil; Wea., weathered granite soil; Fil., filled soil; Gra., gravitational grout; Pre., pressurised grout)

lower than that of gravitational grout before the yield, which means that the shear resistance is stronger during the pullout when the pressurised grout is applied. However, the shear displacement portion of pressurised grout in weathered granite soil, which is denser than the colluvial soil, exhibits behaviour similar to that of gravitational grout before yield. Figure 11(b) shows the variation of the shear displacement portion with respect to the nail length. Obviously, the shear displacement portion decreases when the nail length increases, which means that the longer soil-nail does not allow large shear displacement before and after yield. Figure 11(c) shows the results of filled soil compared with those of weathered granite soil. The shear displacement portion of the 2·0 m nail length installed in the weathered granite soil is smaller than that of the filled soil, which has a 3·0 m nail length. Figure 11(c) also shows that the 3·0 m soil-nail with gravitational grout has a lower shear displacement than the 2·0 m soil-nail with pressurised grout.

In addition, steel and concrete strain gauges were installed in the soil-nail to measure the interaction behaviour between the grout and steel bar, as illustrated in Figures 4(b) and 4(c). In soil-nail design, it is usually assumed that the steel bar moves together with the grout. However, monitoring the results of strain gauges shows that there is a relative strain difference between the grout and the steel bar, as shown in Figure 12(a). The strain of the steel bar is greater than twice that of grout, which means the tensile elongation in the steel bar dominates during the pullout test. However, the loads imposed on the steel bar are similar to those of grout at the same location, as shown in Figure 12(b).

The displacement variation at each location can be estimated from the results of the concrete strain gauges as the pullout load increases (see Figure 13(a)). The displacement increases linearly from the nail tip to the nail head at the initial pullout stages, but it increases significantly between a depth of 1·5 m

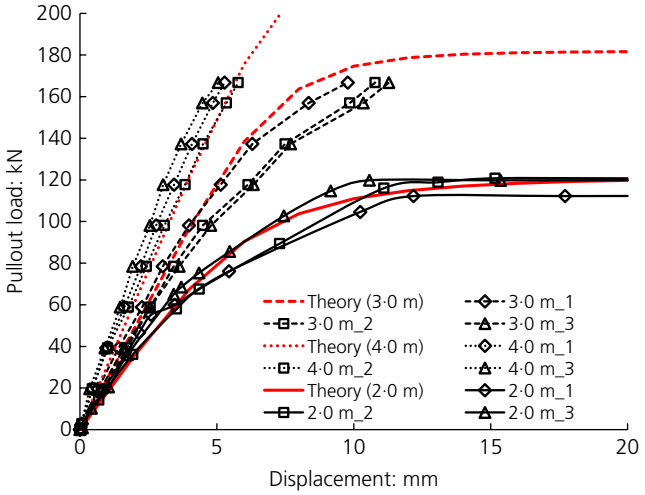

Figure 9. Net load–displacement curve with the variation of bonded length

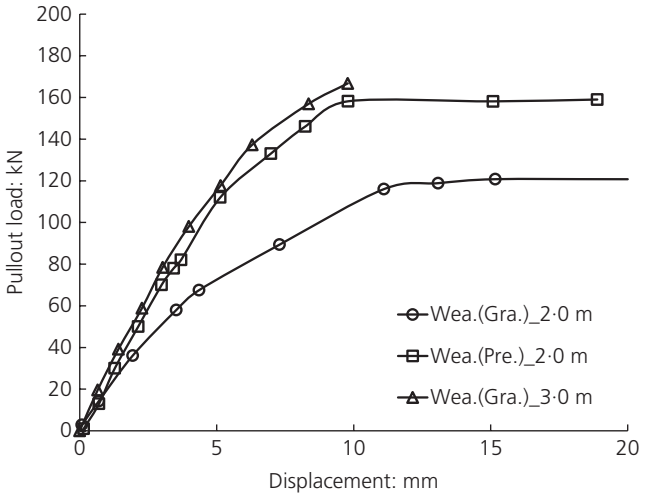

Figure 10. Comparison between pressurised grout and gravitational grout (Wea., weathered granite soil; Gra., gravitational grout; Pre., pressurised grout)

and 3·0 m when the pullout load reaches 98·1 kN. The displacement that occurs in the grout at the nail head is compared with the total displacement in order to compare the grout movement with the total displacement, as shown in Figure 13 (b). Both curves exhibit a linear increase with the increase in the pullout load; the total displacement is almost five times larger than that occurring in the grout. The difference between these two curves represents the shear displacement between the ground and grout, which is almost 80% of the total displacement.

Most soil-nail design methods concentrate on the ultimate limit state (failure). However, it is shown here that the

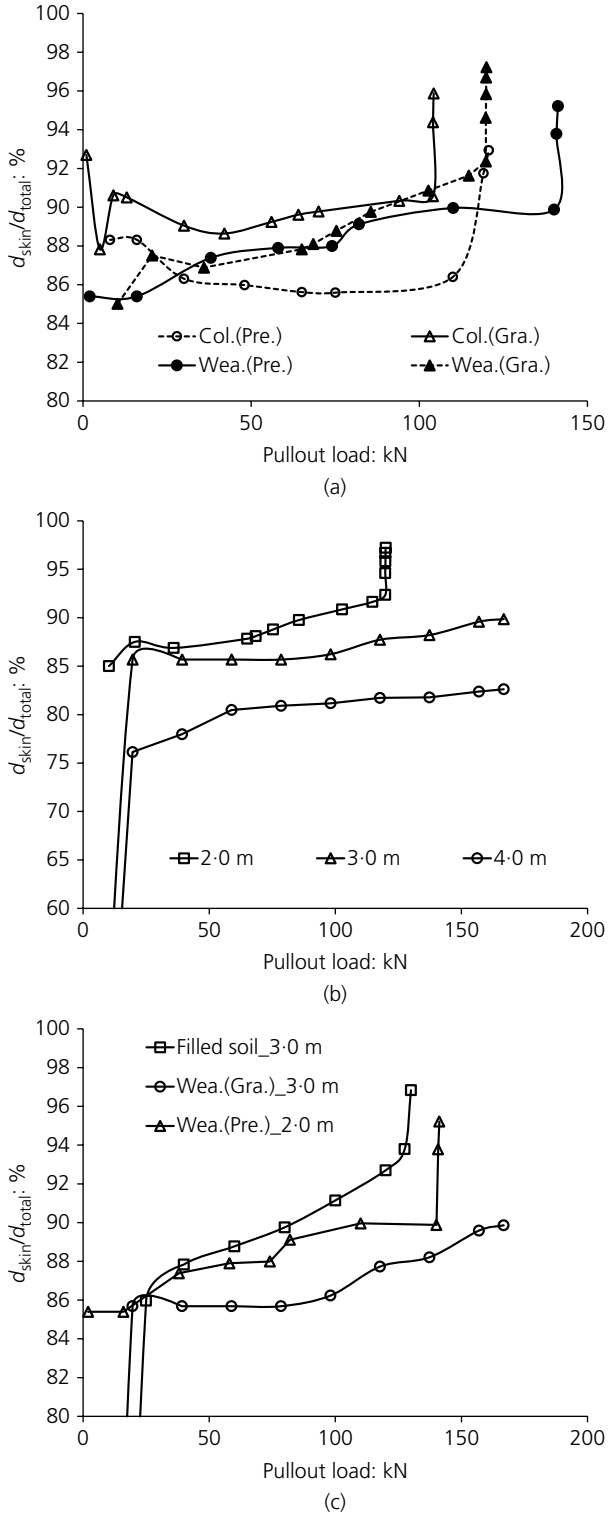

Figure 11. Comparison of shear displacement for the different soils considered (d_{skin}, shear displacement between soil and grout; d_{total}, total pullout displacement): (a) pressurised grout effect; (b) length effect; (c) soil type and pressurised grout effect

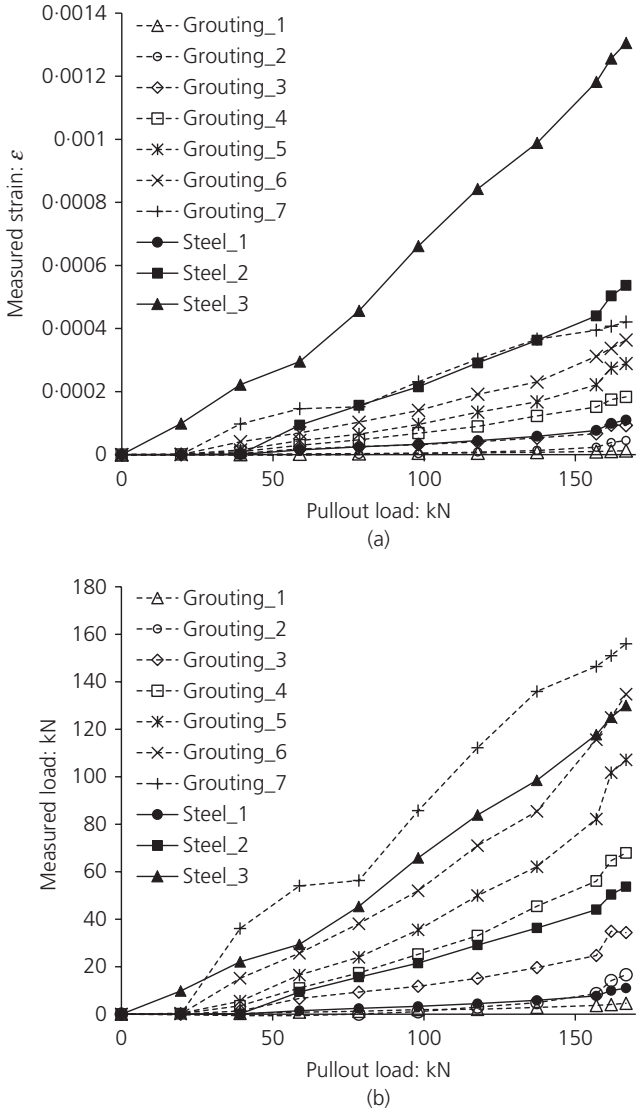

Figure 12. Results of strain measurements: (a) strain variation; (b) load variation

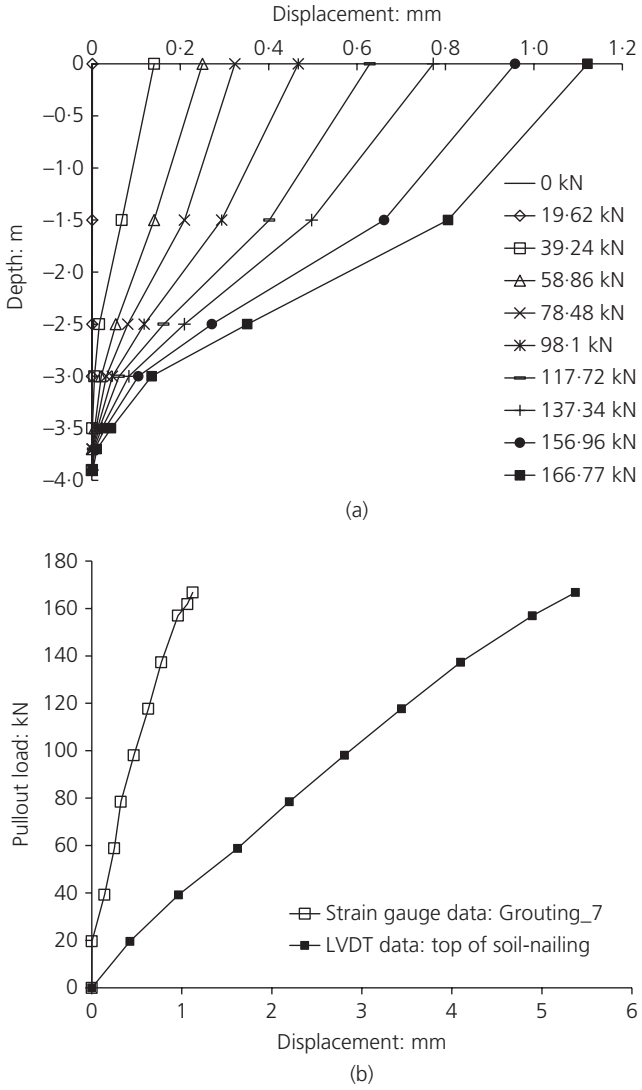

Figure 13. Displacement analysis of soil-nail: (a) displacement variation with depth; (b) displacement at head of soil-nail

displacement of soil-nailed slopes can also be estimated from the soil-nail shear behaviour characteristic.

6. Conclusions

In this research, a combination of analytical studies and real field tests is adopted to determine the shear interaction behaviour between soil, grout and steel bar in the soil-nail system. The importance of this study is that it does not assume a fixity between the steel bar and the surrounding grout, and therefore it considers their relative displacement. The net load–displacement curves are estimated according to ground conditions as well as construction methods. The conclusions are listed below.

(*a*) The slope of the curve was determined by using elastic shear modulus in the theoretical solution to verify the shear behaviour between the ground and the grout. The variation of the curve induced by the grout methods was determined. The limit line of a curve can be determined by the ultimate skin friction theory, and non-linear behaviour can be considered. The theoretical results obtained are compared with field test data; the back-calculated dilatancy angle is obtained to be used as an initial estimate when obtaining the ultimate skin friction by matching two curves.

(*b*) Three different sites and two different construction methods were considered in the investigation. The effect of the grout method was dominant in the results of the net load–displacement curve of each soil. The pullout loads increased by almost 25% in colluvial and weathered granite soils, and the stiffness increased to

almost 40% in all considered soils when pressurised grout was used.

(*c*) The shear displacement portion for pressurised grout is lower than that for gravitational grout before yield, which means that the shear resistance is larger during the pullout when the pressurised grout is applied. The shear displacement portion decreases when the nail length increases, which means that the longer soil-nail does not allow large shear displacement before and after yield.

(*d*) The results of the strains measured both for steel and grout show that the strain experienced by the steel bar is more than twice that in the grout, which means that tensile elongation in the steel bar dominates during the pullout test. The total displacement is approximately five times larger than that occurring in the grout in the displacement analysis. The loads carried by the steel bar are similar to those carried by the grout at the same location.

(*e*) This paper proposed a method to estimate the net load–displacement curve through a combination of established analytical relations and real data from field pullout tests. The results from this study will be useful for estimating the displacement of a soil-nailed structure when the earth structure is sensitive to displacement during the construction stage.

Acknowledgements

This research was supported by a grant (project number: 13SCIP-B066321-01 (Development of Key Subsea Tunneling Technology)) from the Infrastructure and Transportation Technology Promotion Research Program, funded by the Ministry of Land, Infrastructure and Transport of the Korean government. The first author, H. J. Seo, was supported by the Basic Science Research Program through the National Research Foundation of Korea (NRF), funded by the Ministry of Education (no. 2013R1A6A3A03059659).

REFERENCES

JGS (Japanese Geotechnical Society) (2000) JGS4101–2000: Standards for the design and construction of ground anchorages. Japanese Geotechnical Society, Tokyo, Japan.

KISC (Korea Infrastructure Safety Corporation) (2006) *Design Criteria of Slope*. Ministry of Construction and Transportation, Goyang-si, Korea.

NHI (National Highway Institute) (2015) *Soil Nail Walls Reference Manual*. U.S. Department of Transportation, Federal Highway Administration, Washington, DC, USA, FHWA-NHI-14-007.

Pyke RM (1979) Nonlinear soil models for irregular cyclic loadings. *Journal of the Geotechnical Engineering Division, ASCE* **105(GT6)**: 715–726.

Randolph MF and Wroth CP (1978) Analysis of vertical deformation of vertically loaded piles. *Journal of the Geotechnical Engineering Division, ASCE* **104(12)**: 1465–1488.

Seo HJ, Jeong KH, Choi HS and Lee IM (2012) Pullout resistance increase of soil nail induced by pressurized grout. *Journal of Geotechnical and Geoenvironmental Engineering* **138(5)**: 604–613.

Seo HJ, Lee IM and Lee SW (2014) Optimization of soil nailing design considering three failure modes. *KSCE Journal of Civil Engineering* **18(2)**: 488–496.

Tan Y and Chow C (2004) Slope stabilization using soil nails: design assumptions and construction realities. *Proceedings of Malaysia–Japan Symposium on Geohazards and Geoenvironmental Engineering, Bangi, Malaysia*.

Viggiani G and Atkinson JH (1995) Stiffness of fine-grained soil at very small strain. *Géotechnique* **45(2)**: 249–265.

Wang Z and Richwien W (2002) A study of soil–reinforcement interface friction. *Journal of Geotechnical and Geoenvironmental Engineering* **128(1)**: 92–94.